

es because of fluctuations when t is near t_{\max} . By imagining turning the field on at various fixed values of t , one can construct curves similar to those in Fig. 1.

If the simple interpretation given above is accepted, the present experiment shows the existence of a first-order transition in very thin aluminum films at high fields and demonstrates that the extra conductivity above T_c is caused by fluctuations at a second-order transition and not by inhomogeneities.

It is a pleasure to thank Dr. Peter Fulde for helpful suggestions and aid with the data analysis. We also express our gratitude to Mr. Richard MacNabb for making the samples and Mr. Michael Blaho for help in making the measurements.

*Also, Physics Department, Massachusetts Institute of Technology.

†Supported by the U. S. Air Force Office of Scientific Research.

¹V. L. Ginzburg, *Zh. Eksperim. i Teor. Fiz.* **34**, 113 (1958) [*Soviet Phys. JETP* **7**, 78 (1958)].

²A. M. Clogston, *Phys. Rev. Letters* **9**, 266 (1962); B. S. Chandrasekhar, *Appl. Phys. Letters* **1**, 7 (1962). See also R. A. Kamper, R. S. Collier, and Y. Ohori, *Phys. Rev.* **137**, A75 (1965).

³G. Sarma, *J. Phys. Chem. Solids* **24**, 1029 (1963); K. Maki and T. Tsumeto, *Progr. Theoret. Phys.* **31**, 945 (1964); K. Maki, *Progr. Theoret. Phys.* **32**, 29 (1964).

⁴K. Maki, *Phys. Rev.* **148**, 362 (1966); N. R. Werthamer, E. Helfand, and P. C. Hohenberg, *Phys. Rev.* **147**, 295 (1966).

⁵H. Engler and P. Fulde, *Physik Kondensierten Materie* **7**, 150 (1968).

⁶Y. Shapira and L. J. Neuringer, *Phys. Rev.* **140**, A1638 (1965); R. R. Hake, *Phys. Rev. Letters* **15**, 865 (1965); T. G. Berlincourt and R. R. Hake, *Phys. Rev.* **131**, 140 (1963); Y. B. Kim, C. F. Hempstead, and A. R. Strnad, *Phys. Rev.* **139**, A1163 (1965).

⁷R. H. Hammond and G. M. Kelly, *Phys. Rev. Letters* **18**, 156 (1967); H. L. Fine, M. Lipsicas, and M. Strongin, *Phys. Letters* **29A**, 366 (1969).

⁸M. Strongin and O. F. Kammerer, *Phys. Rev. Letters* **16**, 456 (1966).

⁹We are indebted to Dr. N. Blum and Dr. R. Frankel for lending us the He³ cryostat.

¹⁰See, for example, R. E. Glover, *Phys. Letters* **25A**, 542 (1967); M. Strongin, O. F. Kammerer, J. Crow, R. S. Thompson, and H. L. Fine, *Phys. Rev. Letters* **20**, 922 (1968); R. V. D'Aiello and S. J. Freedman, *Phys. Rev. Letters* **22**, 515 (1969); G. Bergman, *Z. Physik* **225**, 430 (1969); L. R. Testardi, W. A. Reed, P. C. Hohenberg, W. H. Haemerle, and G. F. Brenner, *Phys. Rev.* **181**, 800 (1969).

¹¹L. D. Landau and E. M. Lifshitz, *Statistical Physics*, (Pergamon, London, 1958), p. 350.

¹²P. G. de Gennes and M. Tinkham, *Physics* **1**, 107 (1964). These authors showed $1 - [(1-t^2)/(1+t^2)]^{1/3}$ to be very close to the temperature dependence derived from the microscopic theory for a thin film with no paramagnetic limiting.

¹³R. Avenhaus and P. Fulde, *Physik Kondensierten Materie* **5**, 157 (1966).

¹⁴P. Fulde, private communication.

PHONON CONTRIBUTION TO THE FAR-INFRARED ABSORPTIVITY OF SUPERCONDUCTING AND NORMAL LEAD*

R. R. Joyce and P. L. Richards

Department of Physics, University of California, and Inorganic Materials Research Division, Lawrence Radiation Laboratory, Berkeley, California 94720

(Received 16 March 1970)

Low-temperature measurements of the absorptivity of superconducting and normal Pb in the phonon frequency region 15-200 cm^{-1} show an onset of absorption when the photon energy is large enough to excite appreciable numbers of acoustic phonons. The onset begins around the transverse phonon frequency $\Omega \approx 35 \text{ cm}^{-1}$ in the normal metal and around $\Omega + 2\Delta \approx 55 \text{ cm}^{-1}$ in the superconductor. Most features of the data can be explained by a "Golden Rule" calculation of the phonon-generation process proposed by Holstein.

We have measured the far-infrared absorption in single crystals of pure lead over the frequency range from 15 to 200 cm^{-1} in both the superconducting and normal states. These data show the first example of structure on the absorptivity of a metal due to the excitation of phonons. It is

helpful to consider the analogy to the phonon sidebands commonly observed on electronic transitions in insulators. In our case, the "electronic transition" is the excitation spectrum of the normal or superconducting metal, so an increase in absorption due to phonon creation is

expected to start at characteristic phonon frequencies in the normal metal and at the phonon frequencies plus 2Δ in the superconductor. The absorption spectra obtained increase dramatically at the expected frequencies, and structure is observed which can be correlated with peaks in the density of phonon states in Pb. We have thus observed the onset of the volume phonon-generation process proposed by Holstein^{1,2} to account for the near-infrared absorptivity of metals.

In our experiment, radiation from a far-infrared Michelson interferometer³ was focused onto a single-crystal sample of lead about $7 \times 7 \times 0.5$ mm in size, mounted in a highly absorbing cavity. A doped-germanium thermometer was cemented to the back of the sample to monitor its temperature. The sample was supported in the cavity by thin-walled stainless steel tubing which served the dual purposes of thermally isolating the sample and protecting the thermometer from directly absorbing any radiation reflected from the sample. The samples had a residual resistance (R_{300}/R_T) of 13 000 at 4.2°K and 85 000 at 1.2°K. Their surfaces were carefully chemically polished so as to maximize the specular reflection of visible light. The experiments done at 1.2°K on samples in the superconducting state were compared with similar experiments on normal-state lead done in a magnetic field of ~ 1200 G applied parallel to the sample surface. Reference spectra were obtained by substituting a highly absorbing carbon resistance bolometer for the lead sample. Analysis of the data consisted of calculating the ratios of the lead spectra to the carbon bolometer spectrum and the ratio of the superconducting-lead absorption spectrum to the normal absorption spectrum. The superconducting/normal absorption ratios are more useful because any spurious structure due to resonant cavity modes should cancel out of this ratio. The results of many experiments on several samples in two different cavities were averaged and standard deviation confidence levels were computed. No significant differences were observed in the spectra obtained for (100) and (111) sample orientations. This is to be expected since the frequencies are generally too high for the anomalous skin effect to retain appreciable Fermi-surface selectivity.

Figure 1 shows the absorption spectra for superconducting and normal samples normalized to the carbon bolometer. The solid line is the frequency-dependent (surface) absorption arising from the ordinary skin-effect theory. This was

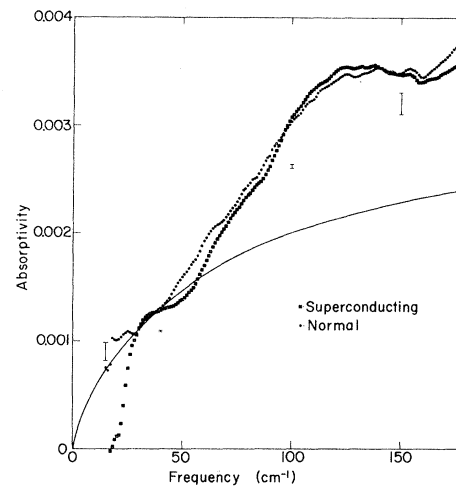


FIG. 1. Measured frequency-dependent absorptivity in superconducting and normal lead compared with the prediction of normal-state anomalous skin-effect theory. The limits of the error bars are plus and minus one standard deviation (75% confidence).

calculated from Dingle's tables⁴ using the relaxation time derived from the resistance-ratio measurement and Chambers's⁵ value of σ/l . The shape of the theoretical curve is not very sensitive to errors in the chosen parameters. The absolute accuracy of the measurements is poor so the scale factor is established by fitting the curves in the region from 20 to 40 cm^{-1} where the theory is expected to be valid.

The spectrum for the superconducting sample shows a well-defined energy-gap absorption edge at 22 cm^{-1} with very little signal at lower frequencies; this indicated that at least 95% of this signal is due to absorption in the lead sample.⁶ In addition, the absorption increases sharply at about 55 cm^{-1} . A similar but less sharp increase begins at about 35 cm^{-1} in the normal sample. Although the onset of the additional volume absorption is slow in the normal state, it must be invoked to explain the fact that the spectrum becomes concave upward. The skin-effect theory predicts a curve which is concave downward throughout this frequency region. These curves show that the Holstein absorption is comparable with the skin-effect absorption for frequencies above the phonon range.

The details of the onset of absorption are seen more clearly in Fig. 2, where the ratio of superconducting to normal absorption is plotted. The ratio rises rapidly from the gap at $2\Delta = 22 \text{ cm}^{-1}$ to a maximum at 35 cm^{-1} . The decrease from 35 to 55 cm^{-1} is due to the absorption onset in the normal spectrum. The ratio then rises in two

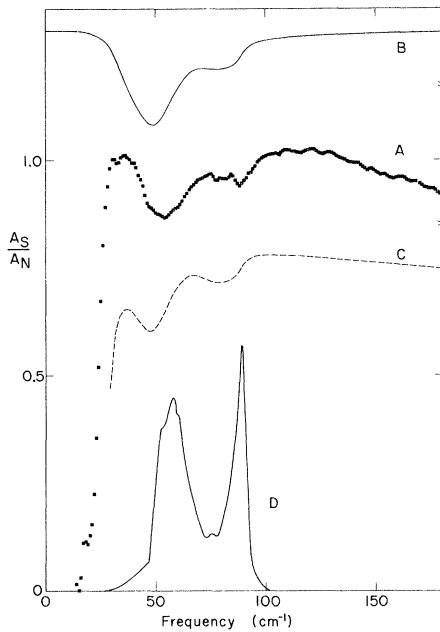


FIG. 2. Measured ratio (curve A) of the absorptivity in superconducting/normal lead compared with (curve B) a theoretical estimate of A_S/A_N which ignores the effect of the energy gap on the superconducting surface absorption, but treats the anomalous skin effect correctly, (curve C) a second estimate of A_S/A_N with the surface absorption taken from the extreme anomalous limit of strong-coupling superconductivity theory, and (curve D) $\alpha^2(\omega-2\Delta)F(\omega-2\Delta)$, the square of the electron-phonon coupling constant times the phonon density of states shifted in frequency by the amount 2Δ . Curves B and C are plotted on the same scale as curve A, but have been shifted vertically for clarity.

steps, centered at ~ 65 and ~ 95 cm^{-1} , which are due to the onset of absorption in the superconducting spectrum.

The accuracy of the data in Fig. 1 decreases toward each end of the measured frequency range. Error bars are shown which indicate that the details of the structure around 150 cm^{-1} are probably not significant. Many errors, both random and systematic, are expected to disappear from the ratio shown in Fig. 2. The data shown there are probably accurate to ± 0.02 . Thus the fine structure near 30 cm^{-1} and beyond 100 cm^{-1} is probably not significant, while some of the sharp features near 85 cm^{-1} may be.

As an independent check of our absorption measurements, we measured the power reaching a bolometer after many reflections in a cavity whose walls were slabs of single-crystal Pb, a cavity used previously to study energy-gap absorption edges in superconductors. The ratio of superconducting to normal absorptivity de-

rived from this experiment was in good agreement with our direct absorption data.

The Holstein process involves the scattering of a conduction electron which simultaneously absorbs a photon and emits a phonon. A rigorous treatment of this process requires a knowledge of the Fermi surface and phonon spectrum of Pb, as well as detailed consideration of the superconducting state. A phenomenological approach suggested by Falicov⁸ can be used, however, to understand the main features of the data. This approach assumes the conduction electrons to be a free-electron gas at $T=0$ and includes energy-conservation but not wave-vector-conservation selection rules. The initial state is a photon of energy ω ; the final state is an electron of energy ϵ_1 , a hole of energy ϵ_2 , and a phonon of energy Ω . The density of final states is assumed to be the convolution of the independent densities of states of the electron, hole, and phonon. The matrix element is assumed constant except for a factor $\omega^{-1/2}$ which arises from the initial photon state, and a possible dependence of the electron-phonon interaction on the phonon frequency. The volume absorptivity is thus proportional to

$$\alpha_v \propto (1/\omega) \int N_e(\epsilon_1) N_h(\epsilon_2) \alpha^2(\Omega) F(\Omega) \times \delta(\epsilon_1 + \epsilon_2 + \Omega - \omega) d\epsilon_1 d\epsilon_2 d\Omega, \quad (1)$$

where N_e and N_h are the electron and hole densities of states, and $\alpha^2(\Omega)F(\Omega)$ is the product of the square of the electron-phonon matrix element and the phonon density of states. Substitution of a constant for the normal electron density of states and a BCS density of states in the superconductor gives the expressions

$$\alpha_{vN}(\omega) \propto (N_0^2/\omega) \int_0^\omega (\omega - \Omega) \alpha^2 F(\Omega) d\Omega, \quad (2)$$

$$\alpha_{vS}(\omega) \propto \frac{N_0^2}{\omega} \int_0^{\omega-2\Delta} \alpha^2 F(\Omega) \times [(\omega - \Omega)E(a) - \frac{2\Delta^2}{(\omega - \Omega)}K(a)] d\Omega, \quad (3)$$

where $E(a)$ and $K(a)$ are complete elliptic integrals with $a^2 = 1 - 4\Delta^2/(\omega - \Omega)^2$. These integrals were calculated using values of $\alpha^2(\Omega)F(\Omega)$ obtained from superconducting tunneling.⁹ A composite spectrum was then calculated by adding the superconducting or normal theoretical Holstein volume absorptivity α_v to the theoretical anomalous skin-effect absorptivity α_s . The ratio of these two absorptivities was estimated by Holstein to be $\alpha_v/\alpha_s = 16\Theta_D \delta_F / 15Tv_F \tau$ in the limit $\hbar\omega \gg k\Theta_D$ where both α_v and α_s are inde-

pendent of frequency. Here δ_r is the high-frequency skin depth c/ω_p , and T is the high temperature, large compared with Θ_D , at which the phonon-limited relaxation time τ is evaluated. The composite absorption in this high-frequency limit has been used successfully to fit the near-infrared absorptivity in copper and silver at low temperatures.¹⁰ Using the experimental value of σ/l and the London penetration depth c/ω_p for Pb,¹¹ we estimate $\alpha_v/\alpha_s \approx 1.9$. A reasonable fit to the data in Figs. 1 and 2, however, requires the smaller² value $\alpha_v/\alpha_s \approx 1$.

The theoretical ratios of the superconducting and normal spectra are compared with the data in Fig. 2. The two curves shown for the theoretical ratio differ by the way in which the conventional skin-effect contribution to the absorption was estimated. In *B* the correct normal-state skin effect from the Dingle tabulation of the theory was used for both the normal and superconducting states. Energy-gap effects on the superconducting skin-effect absorption are ignored. The shape of curve *B* clearly accounts for many of the major features of the data. The computed curve drops smoothly above 35 cm^{-1} as a result of the onset of absorption in the normal state obtained from Eq. (2). It then rises in two steps as a result of the onset of absorption in the superconducting state. The sharply peaked BCS density of electronic states at the energy gap weights the phonon density of states for Ω near $\omega - 2\Delta$. Thus the peaks in $\alpha^2 F(\omega - 2\Delta)$ shown in curve *D* contribute step increases to Eq. (3), and thus to A_S/A_N .

Although qualitatively correct, the structure predicted from our simple model deviates from the measurements in that the latter are systematically broadened and shifted to higher frequencies. For example, the theoretical absorption steps centered at ~ 59 and $\sim 88 \text{ cm}^{-1}$ appear in the measurements at ~ 65 and $\sim 95 \text{ cm}^{-1}$, respectively. This is an understandable consequence of wave-vector selection rules neglected in the theory. Equation (1) implicitly assumes that any electron momentum is available, a good but not perfect approximation for Pb.

In curve *C*, the skin-effect absorption was computed in the extreme anomalous limit from values of $\sigma_1(\omega)$ and $\sigma_2(\omega)$ calculated from strong-coupling superconductivity theory for Pb.¹² The extreme anomalous limit is not accurate for our experimental conditions; it is known, for example, to underestimate the steepness of the onset of A_S above the gap.¹³ The more accurate

wave-vector-dependent calculations of A_S/A_N by Shaw and Swihart¹² are in excellent agreement with the experimental gap edge, but do not extend to the phonon-frequency region. Despite this inaccuracy, curve *C* illustrates two important points. The complex conductivities calculated from strong-coupling superconductivity theory show structure due to virtual phonon effects. This structure appears as small (2-4%) peaks in the skin-effect absorption centered above the peaks in $\alpha^2 F(\omega - 2\Delta)$ (curve *D*). These peaks are small compared with the steps due to real phonon generation and are not identifiable in curve *C* or in the data. A second important effect¹³ (a dispersion in the gap function) causes a broad dip in curve *C* between 100 and 300 cm^{-1} . The fall in the data beyond 120 cm^{-1} may thus be due to strong-coupling effects. Preliminary measurements at higher frequencies show that A_S/A_N continues to fall until 210 cm^{-1} , and then remains constant to 350 cm^{-1} . This shape, but not the magnitude, is in agreement with our approximate theory.

The authors are greatly indebted to Professor L. M. Falicov for suggesting the simple model used to estimate the theoretical Holstein absorption, and to Professor J. C. Swihart for providing values of σ_1 and σ_2 used in calculating the skin-effect absorption. Thanks are also due to Professor M. L. Cohen, Professor D. Scalapino, and Dr. P. Allen for helpful discussions. Our renewed interest in this problem was stimulated by discussions with Dr. H. Scher.

*Work done under the auspices of the U. S. Atomic Energy Commission.

¹T. Holstein, Phys. Rev. **96**, 535 (1954).

²The first known estimate of the onset of Holstein absorption in the normal state was by E. E. H. Shin, Arthur D. Little, Inc., Final Technical Summary Report No. C-62081, 1961 (unpublished). More recently H. Scher, Bull. Am. Phys. Soc. **12**, 672 (1967), has announced a more detailed calculation which appears to fit the experimental magnitude quantitatively.

³R. R. Joyce and P. L. Richards, Phys. Rev. **179**, 375 (1969).

⁴R. B. Dingle, Physica **19**, 311 (1953).

⁵R. G. Chambers, Proc. Roy. Soc. (London), Ser. A **215**, 481 (1952).

⁶Our data are in good agreement with the more recent measurements in the gap region [M. Tinkham, *Optical Properties and Electronic Structure of Metals and Alloys*, edited by F. Abeles (North-Holland, Amsterdam, 1966), pp. 431-451; D. M. Ginsberg and L. C. Hebel, in *Superconductivity*, edited by R. D. Parks (Marcel Dekker, New York, 1969), Vol. 1, pp. 193-

220]. Unfortunately, previous work on bulk samples was not, in general, carried out to high enough frequencies (or with adequate accuracy) to show clearly the Holstein absorption.

⁷P. L. Richards, Phys. Rev. Letters 7, 412 (1961).

⁸L. M. Falicov, private communication.

⁹W. L. McMillan and J. M. Rowell, Phys. Rev. Letters 14, 108 (1965).

¹⁰M. A. Biondi, Phys. Rev. 102, 964 (1956).

¹¹Holstein's estimate can be written $\alpha_V/\alpha_S = 16 \Theta_D \lambda_L / 157l$. We used Chambers's value (Ref. 5) of $\sigma/l = 9.4 \times 10^{10} \Omega^{-1} \text{ cm}^{-2}$, $\lambda_L = 305 \text{ \AA}$ from R. F. Gasparovic and W. L. McLean, to be published, and from handbook values of σT and Θ_D .

¹²W. Shaw and J. C. Swihart, Phys. Rev. Letters 20, 1000 (1968), and private communication, and to be published.

¹³Tinkham, Ref. 6; Ginsberg and Hebel, Ref. 6.

UTILIZATION OF NEAR- AND VACUUM-ULTRAVIOLET SYNCHROTRON RADIATION FOR THE EXCITATION OF VISIBLE FLUORESCENCES IN RUBY AND MgO:Cr³⁺†

W. M. Yen, L. R. Elias,* and D. L. Huber

Department of Physics, University of Wisconsin, Madison, Wisconsin 53706

(Received 16 February 1970; revised manuscript received 26 March 1970)

We report results of studies utilizing ultraviolet synchrotron radiation as a selective excitation source for the *R*-line fluorescence transitions of Cr³⁺ in cubic MgO and Al₂O₃. Pump bands for these fluorescences spanning the near and vacuum ultraviolet are identifiable as charge transfer bands of the CrO₆³⁻ complex. We report the observation of broad bands originating from ligand-to-metal bands and terminating in (3*d*)³ states. Comparison of the excitation spectra of the broad-band fluorescence with that of the *R* lines allows us to assign certain properties to the charge-transfer bands.

The infrared and visible spectra of transition-metal ions doped into ionic hosts have been extensively studied and their general behavior is well understood.¹ This is not the case for their properties in the near and vacuum ultraviolet (uv), principally because of two key difficulties²: (i) Normal laboratory sources are not very intense nor are they continuous throughout this region, and (ii) the host material is generally opaque to radiation at these frequencies making impurity-ion spectroscopic studies difficult, if not impossible, to conduct. The first of these empirical difficulties has been remedied by synchrotron radiation; the recent activity in the field of uv properties of solids attests to the versatility of electron storage-ring synchrotron radiation as an energy source in these hitherto experimentally difficult spectral regions.³

We present in the Letter results of studies where we utilized uv synchrotron radiation as a novel excitation source for visible fluorescence transitions of transition-metal ions doped into some well studied lattices, in particular, Cr³⁺ in cubic MgO and trigonal Al₂O₃. We wish to show that by monitoring the intensity of the well-known ²E_g - ⁴A_{2g} Cr³⁺ transition⁴ as a function of the uv excitation frequency, we are able to probe into the energy level structure of Cr³⁺ and its neighboring anion complex far into the uv, into

regions, in fact, where the host lattice is almost totally opaque to the excitation radiation. We wish to report, as well, observation of intense broad-band and sharp-line fluorescences which have not been reported previously. These fluorescences originate from high-lying metal ion and ligand complexes and allow us to assign certain properties and selection rules to charge transfer bands in Cr³⁺.

Synchrotron radiation from the University of Wisconsin 240-MeV electron storage ring is passed through a $\frac{1}{2}$ -m McPherson model 235 vacuum-uv scanning monochromator; the output is then allowed to irradiate the sample. The samples are rectangular prism shaped and are located in an evacuated chamber ($\leq 10^{-8}$ Torr) in contact with a liquid-nitrogen cold finger. Samples are placed in such a way as to expose a maximum amount of irradiated surface to a viewing port at right angle to the beam. The resulting fluorescences are analyzed through narrow-band filters or through a $\frac{1}{2}$ -m Jarrell-Ash monochromator with scanning capabilities. The intensity of the radiative transition may be monitored as a function of the excitation wavelength or, by switching the uv monochromator to zeroth order, the shape of the fluorescences may be obtained. The number of photons at the output of the uv monochromator were counted directly with a